Measurement of the complex dielectric constant down to helium temperatures. I. Reflection method from 1 MHz to 20 GHz using an open ended coaxial line

H. C. F. Martens, J. A. Reedijk, and H. B. Brom

Citation: Review of Scientific Instruments **71**, 473 (2000); doi: 10.1063/1.1150226
View online: http://dx.doi.org/10.1063/1.1150226
View Table of Contents: http://aip.scitation.org/toc/rsi/71/2
Published by the American Institute of Physics

Measurement of the complex dielectric constant down to helium temperatures. I. Reflection method from 1 MHz to 20 GHz using an open ended coaxial line

H. C. F. Martens,[a] J. A. Reedijk, and H. B. Brom
Kamerlingh Onnes Laboratory, Leiden University, P.O. Box 9504, 2300 RA Leiden, The Netherlands

(Received 25 June 1999; accepted for publication 11 November 1999)

The reflection off an open ended coaxial probe pressed against a material under test is used to determine the complex microwave (1 MHz–20 GHz) dielectric response of the material. A full-wave analysis of the aperture admittance of the probe, in terms of the dielectric properties of the backing material and the dimensions of the experimental geometry, is given. We discuss the calibration procedure of the setup and present the complex dielectric response of several materials determined from the measured reflection coefficient. The results obtained with the open ended coax interpolate well between data taken at lower and higher frequency bands using different experimental methods. We demonstrate that this method can be applied to perform dielectric measurements at cryogenic temperatures. © *2000 American Institute of Physics.*
[S0034-6748(00)04802-4]

I. INTRODUCTION

The study of the dielectric function, $\bar{\epsilon}=\epsilon'-i\epsilon''$, of a given material provides valuable insight in charge-carrier transport and relaxation processes involved.[1–6] For instance, the frequency dependence of the dielectric properties of carbon-black/polymer composites elucidate the morphology of the conductive carbon-black network.[3] Below the optical regime ($f<1$ THz), many features of $\bar{\epsilon}$ are smeared out over decades in frequency, therefore a broadband study is indispensable to extract the electronic and structural information present in the complex permittivity.

At low frequencies, $f=\omega/2\pi<100$ MHz, the wavelength of an applied electromagnetic (EM) signal is generally much larger than any length scale in the experiment. In this case the applied electric field is constant over the size of the sample, and the dielectric properties can be obtained through multiplication of the measured impedance with an appropriate geometrical factor. At higher frequencies, this assumption is no longer valid and the explicit wave character of the applied stimulus must be taken into account. Up to 20 GHz, coaxial lines are suited to transport the EM waves onto a sample. The upper limit results from damping of the signal and higher-mode interference. In the range 10–100 GHz, hollow waveguides are suitable to guide EM waves and to perform dielectric experiments in a narrow band.[7,8] At even higher frequencies (up to 1 THz) quasioptical techniques, as discussed in the subsequent paper[9] (referred to as paper II), are convenient. Cavity perturbation methods work well to obtain the complex permittivity of a sample around a single frequency.[10,11]

The present article focuses on the microwave (MHz–GHz) regime, where several broadband coaxial techniques exist to study the dielectric response of a specimen.[12–14] Often used is the reflection off an open ended coaxial line which is pressed against a sample.[15–20] Since the material under study must be in close contact with the aperture plane of the probe, the open ended coax (OEC) is most suited for dielectric measurements on liquids and soft condensed matter (i.e., polymers, biological tissue). Advantages of this technique are (i) it requires no machining of the sample to fit a measurement cell, (ii) after calibration the dielectric properties of a large number of samples can be routinely measured in a relatively short time span, and (iii) measurements can be performed in a temperature controlled environment.

In the analysis of OEC data, the sample is commonly assumed to be infinitely thick,[17] or the effect of a finite thickness is taken into account by approximate expressions.[18] Here, a full-wave analysis of the aperture admittance of a coaxial line terminated with a medium of finite thickness is given. Dielectric data from 1 MHz to 20 GHz, at room temperature and down to 4 K, obtained with the OEC are presented. The results compare well with dielectric data derived from impedance measurements ($f<10$ MHz), filled waveguide experiments ($f=40$ GHz) and quasioptical experiments ($f=100-500$ GHz).

II. DERIVATION OF THE APERTURE ADMITTANCE

To derive an analytical expression for the aperture admittance of the OEC, we will consider the idealized structure shown in Fig. 1. The configuration consists of a circular coaxial transmission line with inner and outer conductor radii a and b, respectively. The inner and outer conductor are separated by a dielectric having relative dielectric constant ϵ_c. The line is terminated at $z=0$ in a perfectly conducting flange fitted to the outer conductor. The probe is backed by two layers of nonmagnetic media. Medium 1 terminating the line has thickness d and relative permittivity $\bar{\epsilon}_1$, while the second medium with dielectric constant $\bar{\epsilon}_2$ extends to infin-

[a]Electronic mail: martens@phys.leidenuniv.nl

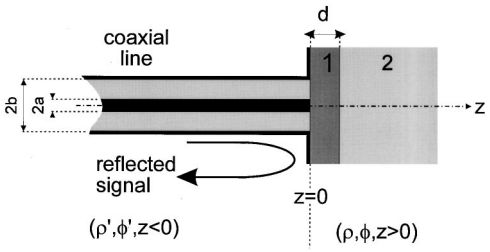

FIG. 1. Configuration of the open ended coax setup. The coaxial line is terminated at $z=0$ in a perfectly conducting flange (ground plane). The probe is backed by two nonmagnetic media with permittivities $\overline{\epsilon_1}$ and $\overline{\epsilon_2}$, respectively. Both the flange and terminating media are laterally unbounded.

ity. Both the ground plane and the terminating media are assumed to be laterally unbounded. The natural choice to make for this geometry is to work with cylindrical coordinates, which we denote as $(\rho',\phi',z\leqslant 0)$ for the coaxial region and $(\rho,\phi,z\geqslant 0)$ for the layered half-space. The aperture admittance can be obtained by matching the electromagnetic fields at the interface $(z=0)$ between the coaxial line and the infinite layered half-space $z\geqslant 0$.[15–17]

We assume that the coaxial line is excited in its principal transverse electromagnetic (TEM) mode, then the fields inside the coaxial region $(z\leqslant 0)$ consist of a superposition of forward traveling and reflected TEM waves and a series of evanescent TM modes stemming from the discontinuity at $z=0$. Due to the azimuthal symmetry of the problem, H_ϕ is the only nonvanishing magnetic component of the EM fields:[15]

$$H_\phi=\frac{A_0}{\rho'}(e^{\gamma_c z}-\Gamma_0 e^{-\gamma_c z})+\sum_{m=1}^{\infty} A_m Z_m(\rho')e^{-\gamma_m z}$$
$$a\leqslant\rho'\leqslant b,\quad z\leqslant 0 \tag{1}$$

with $\gamma_c=i(\omega/c)\sqrt{\epsilon_c}$ the TEM-propagation constant in the coaxial line and Γ_0 the reflection coefficient of the principal TEM mode, A_0 and A_m are measures for the amplitudes of the TEM, respectively, TM modes. The functions $Z_m(\rho')$ (denoting a linear combination of m^{th}-order Bessel functions of the first and second kind) are the orthonormal eigenfunctions of a Bessel differential equation at eigenvalue λ_m^2 and represent the radial distribution of the TM modes. The propagation constant of the damped TM modes is given by $\gamma_m=\sqrt{\lambda_m^2+\gamma_c^2}$. The mathematical properties of these higher order modes are discussed in detail in Refs. 15 and 16. The electrical components of the EM fields follow by application of the Maxwell equation $\nabla\times\mathbf{H}=\epsilon_c\partial\mathbf{E}/\partial t$.

In the case that $d\to\infty$ the field in the half-space $z\geqslant 0$ resulting from the excitation at $z=0$ is given by[15–17]

$$H_\phi(\rho,z)=-\frac{i\omega\overline{\epsilon_1}\epsilon_0}{2\pi}\int_a^b E_{\rho'}(\rho',0)\rho'\,d\rho'$$
$$\times\int_0^{2\pi}\frac{e^{\gamma_1 r}}{r}\cos\phi''\,d\phi'', \tag{2}$$

where $\phi''=\phi-\phi'$ and $r=\sqrt{\rho^2+\rho'^2-2\rho\rho'\cos\phi''+z^2}$ the distance to the source and $\gamma_1=i(\omega/c)\sqrt{\overline{\epsilon_1}}$.

In general, the material under study will have a finite thickness d. The layered geometry will change the EM fields in the region $z>0$ and therefore the aperture admittance. The effect of finite sample thickness has been first examined by Fan and co-workers,[18] who derived the (ω independent) fringing field capacitance of an OEC backed by a layered medium. Jiang *et al.*[19] applied an empirical formulation to take into account the finite thickness of a sample.

The additional interface at $z=d$ partially reflects the EM wave, which is on its turn reflected in the perfectly conducting flange. Repeated application of the image theorem gives a full-wave equation of the EM fields in the region $z>0$:

$$H'_\phi(\rho,z)=\sum_{n=0}^{\infty}\frac{1}{1+\delta_{0n}}\left(\frac{\overline{\epsilon_2}-\overline{\epsilon_1}}{\overline{\epsilon_2}+\overline{\epsilon_1}}\right)^n\times[H_\phi(\rho,z+2nd)$$
$$+H_\phi(\rho,z-2nd)]. \tag{3}$$

This expression is essentially a sum of the fields generated by the stimulus at $z=0$ plus all its induced images at $z=\pm 2dn$; the Kronecker delta symbol δ_{0n} prevents double counting of the original stimulus.

Matching the EM fields Eqs. (1) and (3) at $z=0$ and assuming that the aperture electric field strength is given by the principal TEM mode,[17] the normalized aperture admittance $Y=(1-\Gamma_0)/(1+\Gamma_0)$ evaluates to

$$Y=\frac{2i\omega\overline{\epsilon_1}\epsilon_0}{\left[\ln\left(\frac{b}{a}\right)\right]^2}\sum_{n=0}^{\infty}(2-\delta_{0n})\left(\frac{\overline{\epsilon_2}-\overline{\epsilon_1}}{\overline{\epsilon_2}+\overline{\epsilon_1}}\right)^n$$
$$\times\int_a^b\int_a^b\int_0^{\pi}\frac{e^{\gamma_1 r_n}}{r_n}\cos\phi''\,d\phi''\,d\rho'\,d\rho \tag{4}$$

with $r_n=\sqrt{\rho^2+\rho'^2+4n^2d^2-2\rho\rho'\cos\phi''}$. This integral expression for the aperture admittance can be approximated by making a series expansion of the term $e^{\gamma_1 r_n}$,[17] giving

$$Y\approx Y_1+Y_2+Y_3+Y_4+\cdots,$$
$$Y_1=\frac{2i\omega\overline{\epsilon_1}\epsilon_0}{\left[\ln\left(\frac{b}{a}\right)\right]^2}\sum_{n=0}^{\infty}(2-\delta_{0n})$$
$$\times\left(\frac{\overline{\epsilon_2}-\overline{\epsilon_1}}{\overline{\epsilon_2}+\overline{\epsilon_1}}\right)^n\int_a^b\int_a^b\int_0^{\pi}\frac{\cos\phi''}{r_n}d\phi''\,d\rho'\,d\rho,$$
$$Y_2=0,$$
$$Y_3=-\frac{i\mu_0\omega^3\overline{\epsilon_1}^2\epsilon_0^2}{\left[\ln\left(\frac{b}{a}\right)\right]^2}\sum_{n=0}^{\infty}(2-\delta_{0n})$$
$$\times\left(\frac{\overline{\epsilon_2}-\overline{\epsilon_1}}{\overline{\epsilon_2}+\overline{\epsilon_1}}\right)^n\int_a^b\int_a^b\int_0^{\pi}\cos\phi''r_n\,d\phi''\,d\rho'\,d\rho, \tag{5}$$
$$Y_4=\frac{\mu_0^{3/2}\omega^4\overline{\epsilon_1}^{5/2}\epsilon_0^{5/2}}{3\left[\ln\left(\frac{b}{a}\right)\right]^2}\sum_{n=0}^{\infty}(2-\delta_{0n})$$
$$\times\left(\frac{\overline{\epsilon_2}-\overline{\epsilon_1}}{\overline{\epsilon_2}+\overline{\epsilon_1}}\right)^n\int_a^b\int_a^b\int_0^{\pi}\cos\phi''r_n^2\,d\phi''\,d\rho'\,d\rho.$$

Since Y_1 is essentially a product of ω, a combination of $\bar{\epsilon}_1$ and $\bar{\epsilon}_2$, and geometrical factors, it corresponds to the (frequency independent) fringing field capacitance as was also calculated by Fan *et al.*,[18] and which is a good approximation for the low frequency admittance. The second term is only dependent on the integration variables through $\cos\phi''$ and consequently goes to zero upon angular integration. The third term is a ω dependent correction to the fringing field capacitance; Y_4 can be associated with radiation loss and does not depend on d. The threefold integrals in Eq. (5) only depend on the geometry of the problem and can be evaluated numerically; depending on the dielectric constants of sample and backing medium the sums can be truncated at a finite n. In the present study, the integrals were determined to an accuracy of 10^{-4}, and the sums could be truncated above $n=10$. When the dielectric properties of the backing layer ($\bar{\epsilon}_2$) are known, the sample permittivity $\bar{\epsilon}_1$ can be derived from the measured aperture admittance.

III. CALIBRATION PROCEDURE

Experimentally, the aperture admittance is derived from the measured reflection coefficient Γ_m at the analyzer port. In general, Γ_m will differ from the reflection coefficient at the aperture plane, Γ_0, due to imperfection and finite length of the connections between the probe and measurement apparatus. At a single frequency, the relationship between the measured reflection coefficient and aperture admittance can be expressed as

$$Y=\frac{a\Gamma_m+b}{c\Gamma_m+1}. \tag{6}$$

The coefficients a, b, and c can be determined from the measurement of three reference materials with accurately known dielectric properties. Commonly, two of these references are an open and a short circuit, while the third reference should preferably be chosen in the expected $\bar{\epsilon}$ range of the sample. However, as the parameters a, b, and c (which actually describe the impedance transformation occuring between the analyzer port and measurement plane) are independent of the aperture admittance, the use of any three well defined standards suffices to extrapolate a measured reflection coefficient to the experimental (sample) aperture admittance.

Unfortunately, it is widely recognized that materials having their dielectric response characterized to the degree necessary for calibration purposes are rare. By taking more standards, this problem can be circumvented and an improved calibration of the probe can be obtained; here we follow the suggestions of Evans and Michelson.[20] Since the admittance of a short circuit Y_{sh} is always orders of magnitude larger than any other available standard, the calibration procedure can be simplified by taking $Y_{sh}\to\infty$ from which it follows that $c=-1/\Gamma_{sh}$. The remaining two parameters can be obtained from a linear regression procedure. Using a variety of dielectric standards an accurate calibration of the OEC is possible.

For the open calibration the OEC is kept in air; a slab of indium was found to give a good and reproducible short circuit. For the remaining calibration measurements we have several highly purified reference liquids at our disposal, together with well characterized solids like teflon, sapphire, and quartz. In our opinion, the dispersion-less (up to GHz frequencies) standards toluene, quartz, teflon, and sapphire are more reliable. Among the most accurately defined polar liquids are water[21] and the primary alcohols[22,23] (see Ref. 20 for a more extensive list of reference liquids). However, dielectric data of sufficient accuracy are scarce. Therefore extensive measurements were carried out to obtain a satisfactory description of the standards employed in our study. To describe the response of the polar liquids, the Cole–Cole formula[24] $\bar{\epsilon}=\epsilon_\infty+(\epsilon_s-\epsilon_\infty)/[1+(i\omega\tau)^\alpha]$ is used, where ϵ_s and ϵ_∞ represent the static, respectively, high frequency dielectric constant, τ is the average dipolar relaxation time and α is a measure for the distribution in relaxation times. The parameters used to characterize the standards in the present study are listed in Table I, and compare well with literature values.

TABLE I. Empirical parameters describing the dielectric repsonse {using the Cole-Cole formula (Ref. 24) $\bar{\epsilon}=\epsilon_\infty+(\epsilon_s-\epsilon_\infty)/[1+(i\omega\tau)^\alpha]$} at 293 K of the reference materials used in the calibration of the OEC probe.

Reference material	ϵ_s	ϵ_∞	τ [ps]	α
methanol	34.3	4.86	55.3	0.01
ethanol	25.6	4.33	173.0	0.00
2-propanol	19.5	3.33	382.0	0.02
1-octanol[a]	10.71	3.31	1495.0	0.00
	3.31	2.54	64.6	0.00
quartz	3.81	⋯	⋯	⋯
toluene	2.39	⋯	⋯	⋯
teflon	2.06	⋯	⋯	⋯
sapphire	9.4	⋯	⋯	⋯

[a]The dielectric data of 1-octanol are fitted with two overlapping Debye dispersions.

Due to the relatively simple configuration of the OEC, the measurements can be easily extended to a temperature-controlled environment. However, several experimental problems arise that must be paid attention to. First, when cooling, care must be taken to keep physical contact between the sample and measurement plane of the probe down to the lowest temperatures. This can be achieved by pressing the sample very tight by to the probe using for instance a clamping construction. A problem that can be encountered with the semirigid lines is shrinkage of the inner conductor compared to the outer conductor due to which the electrical contact with the sample gets lost. We circumvented this problem by building a small rigid probe supplied with a (SMA) connector which is attached to the end of a rigid coax by means of a counter connector, see Fig. 2. We encountered no difficulties in cooling these connections down to 4 K. Another point of concern is the calibration of the setup. Due to thermal shrinkage of the coaxial line the electric delay of the experimental setup changes. Furthermore, line loss due to skin resistance decreases upon cooling, giving a higher absolute value of the reflected signal. To correct for these effects, it is necessary to perform at least one three-point calibration at the desired temperature. Using short, open, and quartz stan-

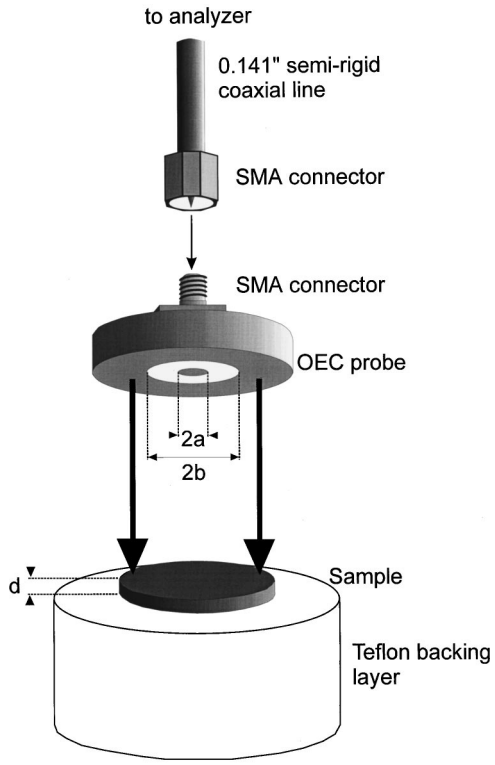

FIG. 2. Schematic drawing of the insert designed for the low temperature OEC measurements. The probe is attached by means of a SMA connection to a cryogenic semirigid coaxial line which transports the signal to the analyzer. The outer diameter of the probe is 16.0 mm, while the inner and outer conductor dimensions are $2a=1.27$ and $2b=4.13$ mm, respectively. The probe is pressed against the sample which is placed on a thick piece of teflon. A clamping construction was used to affirm good contact between the measurement plane and sample down to the lowest temperatures.

dards dielectric measurements at GHz frequencies were made down to 4 K.

IV. EXPERIMENTAL RESULTS

For the experiments presented here a probe was constructed based on a teflon-filled coaxial line with $2a=1.27$ mm and $2b=4.13$ mm, fitted with a flange of 3 cm diameter. The backing material consists of a teflon cylinder ($\overline{\epsilon_2}=2.06+0.00i$). The dimensions (30 mm diameter and a length of at least 30 mm) were sufficiently large to mimic an infinite medium. The teflon cylinder also serves to press the sample against the OEC. Typical dimensions of solid samples studied are $d\sim 0.5-5$ mm and diameter of the order of 1–2 cm.

The low temperature data were taken with a similar probe with a somewhat smaller flange attached to a 0.141 in. cryogenic semirigid coaxial cable as is shown in Fig. 2. A clamping construction was used to ensure good electrical contact between the probe and sample; no contact problems occured down to 4 K. Temperature variation between 4 and 300 K was achieved in an Oxford-Instruments flow cryostat. The temperature was measured using a RhFe thermometer mounted close to the sample, during a single measurement the temperature remained stable within 0.5 K. Reflection data were taken with a HP4291A in the range 1 MHz–1.8 GHz, between 50 MHz and 13.5 GHz a HP8719D was used, and from 8 to 18 GHz the experiments were performed with an ABmm MVNA.

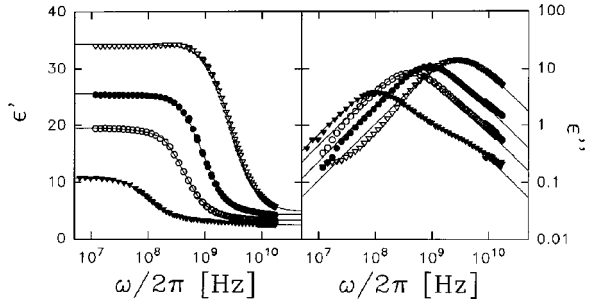

FIG. 3. Real and imaginary part of the dielectric function in the range 10 MHz–20 GHz of methanol (open triangles), ethanol (dots), 2-propanol (open circles), and 1-octanol (closed triangles) obtained with an open ended coaxial probe. The solid lines are fits to the empirical Cole-Cole equation, see Table I.

In Fig. 3, room temperature dielectric data obtained with the OEC on 1-octanol, 2-propanol, ethanol, and methanol are plotted. Data taken with different analyzers are in excellent mutual agreement. The solid lines represent the theoretical curves according to the values listed in Table I. An example of a measurement on a solid material is shown in Fig. 4. The real part of the dielectric permittivity ϵ' and the alternating-current (ac) conductivity $\sigma'=\omega\epsilon_0\epsilon''$ of an agglomeration of dielectric spheres coated with a conducting layer was measured over a broad frequency range.[6] The data taken with the OEC (black dots) interpolate well with the results of standard impedance measurements in a sandwich configuration ($f<10$ MHz) and data obtained from measurements in a rectangular waveguide (40 GHz) and quasioptical measurements (100–500 GHz) on the same sample. The same is true for the OEC measurements on a carbon-black/polymer composite in the range 4–300 K, see Fig. 5 and paper II. Using open, short, and quartz calibration standards accurate dielectric measurements at GHz frequencies can be performed down to the lowest temperatures.

V. DISCUSSION

In the frequency range 1 MHz–20 GHz, accurate and reproducible dielectric measurements can be performed with

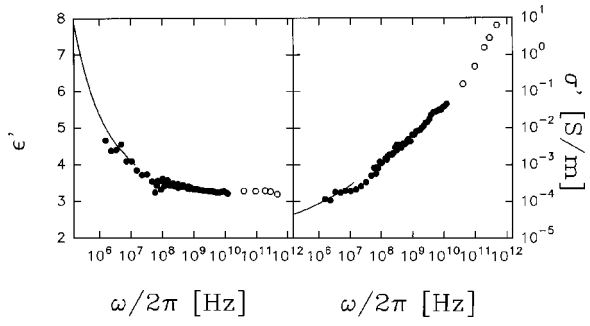

FIG. 4. Dielectric constant ϵ' and conductivity $\sigma'=\omega\epsilon_0\epsilon''$ of an agglomeration of dielectric spheres coated with a conducting layer (Ref. 6). The dots are data obtained with the OEC. The results overlap well with data taken at low frequency (impedance measurement, drawn line) and high frequency (filled waveguide and quasioptical method, circles).

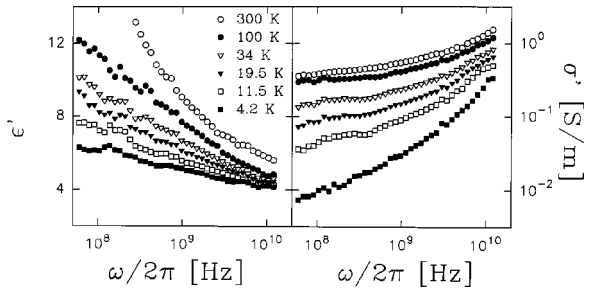

FIG. 5. Temperature and frequency dependence of the dielectric permittivity ϵ' and conductivity $\sigma' = \omega\epsilon_0\epsilon''$ of a carbon-black/polymer composite with the conductive filler concentration above the percolation threshold ($p = 1$ vol %) (Ref. 3). Using the OEC technique accurate dielectric measurements at GHz frequencies can be made down to liquid helium temperatures.

the open ended coax technique. At the low frequency side the technique is limited due to the vanishingly small differences in the measured reflection coefficient for different materials or standards. Especially for low-loss samples, the uncertainty in ϵ'' becomes large below 100 MHz. In the range 0.1–20 GHz the complex dielectric constant can be obtained within an absolute accuracy $\Delta\overline{\epsilon} < 0.1$. At high frequencies the technique is limited due to the limitations of the coaxial guides.

When measuring solid samples in some cases at low frequencies, $f < 100$ MHz, contact problems lead to severe systematic errors: an apparently too high ϵ' and too low ϵ''. These problems can be overcome by application of suitable metallic contacts on the specimen. Surface roughness of the probe interface can yield small air gaps between the sample and coaxial line resulting in similar systematic errors. When measuring liquids such imperfectness is usually less significant.

Another important source of error can be the calibration procedure. Specifically, inaccurate characterization of polar standards can lead to large systematic errors. For instance, a too low estimate of the relaxation time τ of a polar standard gives rise to systematic deviations of ϵ_1'': too low (or even negative) at $\omega < \tau^{-1}$ and too high for $\omega > \tau^{-1}$. These errors are easily recognized due to the resulting peculiar ''wavy'' shape in the derived $\epsilon_1'(\omega)$ and $\epsilon_1''(\omega)$. Typically, we find that uncertainties in τ of the order 10%–50% and in ϵ_s and ϵ_∞ of the order of 10% of the polar standards (which are common discrepancies found in the literature values) can lead to $|\Delta\overline{\epsilon}| \approx 1$, hence these errors are most severe for low $\overline{\epsilon}$ samples. By using a variety of well characterized reference materials (uncertainty no more than a few percent) the calibration parameters a, b, and c can be accurately determined and these systematic errors can be reduced to a few percent. A related problem is contamination of the reference liquids which can also yield significant errors. Therefore, the highly purified liquids were only used a few times for calibration purposes. Furthermore, only after careful cleaning the probe was immersed in the reference liquids.

Finally, attention must be given to the rigidity of the experimental setup. Changes in the (position of the) connecting lines, connectors or probe and drift in the measurement apparatus can render a previously performed calibration useless. These problems are circumvented by using a rigid experimental setup and performing the sample measurements directly after the calibration procedure. Flexing of the lines during measurement and calibration procedure is avoided, and care is taken to tightly fit all connectors. As a check up, several open circuits are taken during a measurement cycle which are afterwards inspected for mutual correspondence.

In summary, over the full frequency range 1 MHz–20 GHz ϵ' can be accurately determined. Below 100 MHz for small ϵ'' values the OEC is not accurate and impedance measurements are more suited to determine ϵ''.

ACKNOWLEDGMENTS

The authors thank I.-P. Faneyte, L. J. Adriaanse, and J. A. J. M. Disselhorst for their respective contributions to the present work. This work is part of the research program of Stichting FOM which is part of the Dutch Science Organization NWO.

[1] A. Fizazi, J. Moulton, K. Pakbaz, S. D. D. V. Rughooputh, P. Smith, and A. J. Heeger, Phys. Rev. Lett. **64**, 2180 (1990).
[2] R. Pelster, G. Nimtz, and B. Wessling, Phys. Rev. B **49**, 12718 (1994).
[3] L. J. Adriaanse, J. A. Reedijk, P. A. A. Teunissen, H. B. Brom, M. A. J. Michels, and J. C. M. Brokken-Zijp, Phys. Rev. Lett. **78**, 1755 (1997).
[4] J. A. Reedijk, L. J. Adriaanse, H. B. Brom, L. J. de Jongh, and G. Schmid, Phys. Rev. B **57**, 15116 (1998).
[5] J. Planès, E. Bańka, R. Senis, and A. Proń, Synth. Met. **84**, 797 (1997); J. Planès, A. Wolter, Y. Cheguettine, A. Proń, F. Genoud, and M. Nechtstein, Phys. Rev. B **58**, 7774 (1998).
[6] O. Hilt, H. C. F. Martens, J. A. Reedijk, H. B. Brom, and P. J. P. Jansen, Synth. Met. **102**, 1149 (1999).
[7] S. Shridar, D. Reagor, and G. Gruner, Rev. Sci. Instrum. **56**, 1946 (1985).
[8] J. Joo and A. J. Epstein, Rev. Sci. Instrum. **65**, 2653 (1994).
[9] J. A. Reedijk, H. C. F. Martens, B. J. G. Smits, and H. B. Brom, Rev. Sci. Instrum. **71**, 478 (2000).
[10] P. K. Yu and A. L. Cullen, Proc. R. Soc. London, Ser. A **380**, 49 (1982).
[11] H. H. S. Javadi, K. R. Cromack, A. G. MacDiarmid, and A. J. Epstein, Phys. Rev. B **39**, 3579 (1989); Z. H. Wang, E. M. Scherr, A. G. MacDiarmid, and A. J. Epstein, Phys. Rev. B **45**, 4190 (1992).
[12] N.-E. Behladj-Tahar and A. Fourrier-Lamer, IEEE Trans. Microwave Theory Tech. **MTT-34**, 346 (1986).
[13] N.-E. Behladj-Tahar, A. Fourrier-Lamer, and H. de Chanterac, IEEE Trans. Instr. Meas. **39**, 4190 (1992).
[14] D. Vincent, L. Jorat, J. Monin, and G. Noyel, Meas. Sci. Technol. **5**, 990 (1994).
[15] H. Levine and C. H. Papas, J. Appl. Phys. **22**, 29 (1951).
[16] J. Galejs, *Antennas in Inhomogeneous Media* (Pergamon, Oxford, 1969), Chap. 3, p. 33.
[17] D. K. Misra, IEEE Trans. Microwave Theory Tech. **MTT-35**, 925 (1987).
[18] S. Fan, K. Staebell, and D. Misra, IEEE Trans. Instr. Meas. **39**, 435 (1990).
[19] G. Q. Jiang, W. H. Wong, E. Y. Raskovich, W. G. Clark, W.A. Hines, and J. Sanny, Rev. Sci. Instrum. **64**, 1614 (1993).
[20] S. Evans and S. C. Michelson, Meas. Sci. Technol. **6**, 1721 (1995).
[21] U. Kaatze and V. Uhlendorf, Z. Phys. Chem., Neue Folge **126**, 151 (1981).
[22] F. Buckley and A. Maryott, *Tables of Dielectric Dispersion Data for Pure Liquids and Dilute Solutions* (U.S. EPO, Washington, DC, 1958).
[23] B. P. Jordan, R. J. Sheppard, and S. Szwarnowski, J. Phys. D: Appl. Phys. **11**, 695 (1978).
[24] K.S. Cole and R.H. Cole, J. Chem. Phys. **9**, 341 (1941).